

CCT Nodes Anchored by Headed Bars— Part 2: Capacity of Nodes

by M. Keith Thompson, James O. Jirsa, and John E. Breen

The anchorage behavior of headed reinforcement in CCT nodes was studied experimentally. A model for the capacity provided by head bearing was developed using a broad database collected from studies of headed reinforcement, deeply embedded anchor bolts, and bearing strength tests of concrete blocks. The proposed model has similarities to existing side blowout and bearing strength formulas.

Keywords: anchorage; bars; reinforcement.

INTRODUCTION

The Texas Department of Transportation (TxDOT) funded a program to study the feasibility of headed reinforcement in bridge structures. An experimental program focusing on the behavior of headed reinforcing bars in CCT nodes was developed. A companion study also examined the behavior of headed reinforcement in lap splices. This report is the second of a two-part article and deals solely with the results of the CCT node study. In Part 1,¹ the mechanics of CCT nodes and anchorage of headed reinforcement were discussed. In Part 2, the capacity of unconfined nodes anchored by headed reinforcement is presented and a model for the anchorage capacity of headed bars is developed.

Results from Part 1¹ that are important to this paper are repeated here:

1. CCT nodes failed in modes related to anchorage of the tie bar. Failure at the node resulted in immediate rupture of adjacent struts;
2. The anchorage capacity of headed reinforcement consisted of head-bearing and bond components. As stress was initially placed on a headed bar, the force was carried predominantly by bond. Bond stresses, however, eventually reached peak capacity and then began to decrease. Subsequent increases in bar stress were transferred to the head causing stress at the head to increase as bond stress decreased. At failure, anchorage capacity was provided by peak head bearing plus reduced bond; and
3. The magnitude of bond stress at failure decreased in relation to increasing relative head area (relative head area was defined in Part 1 as the ratio of net head bearing area to bar area, A_{nh}/A_b).

The capacity of CCT nodes anchored by headed reinforcement can be dealt with in several ways. The node and adjacent struts can be analyzed using the provisions of Appendix A of ACI 318-02.² These provisions treat node capacity as a function of compression stress on the faces of the node and struts. These provisions also require that sufficient anchorage length be provided to develop the tie bar in tension. Thus, the provisions of Appendix A address two modes of failure at the node: overstress of the node in compression and failure of the anchorage between the tie and the node. In the case of headed bar anchorage of a tie, two components must be dealt with at failure: bearing of the head and bond.

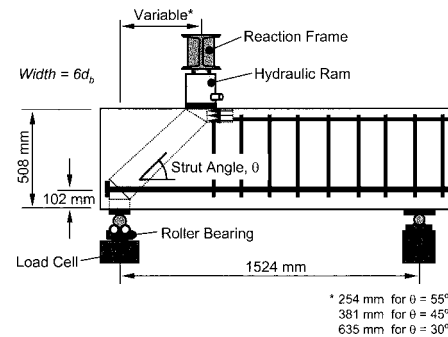


Fig. 1—Typical CCT node test specimen.

Because the bearing face of the head will also be a face of the nodal zone, there is some overlap between the two failure modes when headed reinforcement is used.

The ACI code does not present definitive criteria for the capacity of headed reinforcement. There are existing provisions, however, that may be applicable for treating head bearing and bond separately. Appendix D of 318-02 provides criteria for capacity of headed anchors. DeVries et al.^{3,4} found that deeply embedded headed bars fail by side blowout and recommends a model similar to that provided in ACI 318, Section D.5.4, for side blowout of deeply embedded anchors. The side blowout provisions provide one model for the head-bearing component of anchorage. Another model for head bearing can be found in ACI 318, Section 10.17, “Bearing Strength.” The bond component can be modeled using the development length formula provided in ACI 318, Section 12.2, “Development of Deformed Bars and Deformed Wire in Tension.” If separate models can be found for bond and head-bearing components, total anchorage is potentially the sum of the two.

RESEARCH SIGNIFICANCE

Sixty-four CCT node specimens were tested. The experimental data can be compared to several existing approaches for determining the capacity of nodes and anchorage capacity of headed reinforcement. Attributes of the various methods are discussed and recommendations for determining the capacity of CCT nodes are proposed.

TEST PROGRAM

A typical CCT node specimen is shown in Fig. 1. (Details of the specimen were discussed in Part 1¹ and further

ACI Structural Journal, V. 102, No. 6, November-December 2005.

MS No. 04-304 received September 24, 2004, and reviewed under Institute publication policies. Copyright © 2006, American Concrete Institute. All rights reserved, including the making of copies unless permission is obtained from the copyright proprietors. Pertinent discussion including author's closure, if any, will be published in the November-December 2006 *ACI Structural Journal* if the discussion is received by July 1, 2006.

ACI member **M. Keith Thompson** is an assistant professor at the University of Wisconsin-Platteville, Platteville, Wis. He received his BS from North Carolina State University, Raleigh, N.C., and his MS and PhD from The University of Texas at Austin, Austin, Tex. His research interests include anchorage of reinforcement and strut-and-tie modeling.

James O. Jirsa, FACI, holds the Janet S. Cockrell Centennial Chair in Engineering at the University of Texas at Austin. He is a Past President of ACI, a member of the ACI Board of Direction, and a Past Chair of the Technical Activities Committee. He is a member of ACI Committees 318, Structural Concrete Building Code; 408, Bond and Development of Reinforcement; and is a member and Chair of Subcommittee 318-F, New Materials, Products, and Ideas.

ACI Honorary Member **John E. Breen** holds the Nasser I. Al-Rashid Chair in Civil Engineering at the University of Texas at Austin. He is a member and Past Chair of ACI Committee 318, Structural Concrete Building Code; is a member of ACI Committees 318-B, Reinforcement and Development; 318-E, Shear and Torsion; 355, Anchorage to Concrete; and is a Past Chair of the Technical Activities Committee.

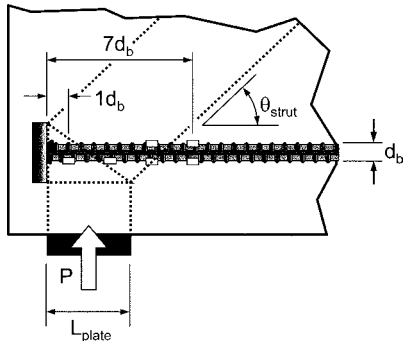


Fig. 2—Detail of CCT nodal zone.

information can be found in Reference 5.) Results of the 64 CCT node tests are summarized in Table 1. The significant variables of each specimen, capacity, and mode of failure are listed. Several of the variables are illustrated in Fig. 2. Three values of capacity are listed: the maximum bearing reaction at the node P_{max} , the bar stress corresponding to this load at the head (located at $1d_b$ from the face of the head), and the bar stress at seven diameters $7d_b$ from the face of the head (the approximate location of the end of the extended nodal zone in most specimens). The failure modes of the CCT nodes are briefly explained below:

- Pullout—pullout of the tie bar from the node without significant rupture of the node concrete.
- Splitting—rupture of the concrete at the node with lateral splitting predominant.
- Crushing—rupture of the concrete at the node with crushing predominant.
- Yield—tie bar yielding before failure of the node.

Although 64 total specimens were tested, many failed in a manner that precluded their use in evaluating models for node capacity. Several specimens used to develop the procedures of the test program were excluded. Tests in which the tie bar yielded were also excluded as were confined tests and tests with hooked bars. The remaining 31 specimens are listed in Table 2.

Analysis of node and strut stress limits

Two modes of failure were examined: overstress of the node at a critical face and overstress of the strut at a critical face. The recommendations of Appendix A of ACI 318² were used to calculate theoretical capacities that were compared to the experimental data. The bearing stress at the head was determined for 26 tests and compared to the nodal stress limit. Nonheaded bars were excluded (Tests 1, 10, 21,

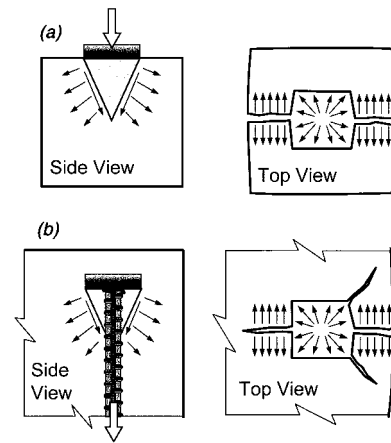


Fig. 3—Comparison of: (a) bearing failure; and (b) side blowout.

and 23 from Table 2) as well as one test in which critical data was not recorded (Test 19). The resultant stress at the strut face calculated for 25 tests and compared with the strut stress limit. Nonheaded bars were excluded (Tests 1, 10, 21, and 23) as well as two tests in which the critical data was not recorded (Tests 11 and 12). For both failure modes, the recommendations of Appendix A provided significant underestimations of capacity with much scatter in the precision. The ranges, means, and coefficients of variation for ratios of measured-to-calculated strength for these failure modes are given in Table 3. Additional details of these analyses can be found in Reference 5.

Analysis of capacity models for head bearing

Two models were examined: the side blowout provisions of ACI 318, Section D.5.4,² and the bearing strength provisions of ACI 318, Section 10.17.² Both models provided more accurate results than the strut-and-tie provisions of Appendix A. Both models were used to calculate the maximum bar stress at the head that should occur before failure. These calculated values were compared to 26 tests from the CCT node database. Non-headed bars were excluded (Tests 1, 10, 21, and 23) as well as Test 19 because critical data was lacking. The side-blowout model tended to underestimate capacity and provided comparatively good precision. The side-blowout mode was conservative for all but four tests. The bearing model tended to slightly overestimate capacity and also had similar precision to the side-blowout model. The bearing model was unconservative for 13 tests. The ranges, means, and coefficients of variation of these models are given in Table 3. Additional details of these analyses can be found in Reference 5.

Development of model for bearing capacity

In addition to examining existing models for head-bearing capacity, development of a new model was explored. Both the side-blowout and bearing-strength models depend on similar variables: cover dimension c and the square root of bearing area $\sqrt{A_{nh}}$. Both models are related to concrete strength f'_c but use different powers (f'_c for bearing and $\sqrt{f'_c}$ for side blowout). The side-blowout model, however, contains a relationship to the ratio c/c_2 that the bearing model does not contain. In exploring an improved model for head-bearing capacity, the same variables were used. The proposed model is a hybrid of the existing models: a power

Table 1—Summary of CCT node tests

	Head dimensions, mm*	θ_{strut} , degrees	d_b , mm	L_{plate}/d_b	A_{nh}/A_b	c/d_b	c_2/d_b	f'_c , MPa	f_s at $1d_b$, MPa	f_s at $7d_b$, MPa	P_{max} , kN	Failure mode
Trial tests	No head	45	25	6.0	0.00	4.0	4.0	39	—	—	—	Shear [†]
	$d_h = 38$	45	25	6.0	1.18	4.0	4.0	39	—	—	285	Shear [†]
	76 x 38	45	25	6.0	4.70	4.0	4.0	39	—	—	239	Shear [†]
	76 x 76	45	25	6.0	10.39	4.0	4.0	39	—	—	334	Shear [†]
	No head	45	25	6.0	0.00	4.0	4.0	21	—	—	201	Pullout
	$d_h = 38$	45	25	6.0	1.18	4.0	4.0	21	—	—	230	Splitting
	76 x 38	45	25	6.0	4.70	4.0	4.0	21	—	—	338	Crushing
	76 x 76	45	25	6.0	10.39	4.0	4.0	21	—	—	322	Crushing
	No head	45	25	6.0	0.00	3.0	4.0	21	—	—	217	Pullout
	76 x 38	45	25	6.0	4.70	3.0	4.0	21	—	—	297	Crushing
	76 x 76	45	25	6.0	10.39	3.0	4.0	21	—	—	257	Crushing
	No head	45	25	6.0	0.00	3.0	4.0	28	112	385	239	Pullout
	No head	55	25	4.0	0.00	3.0	4.0	27	81	346	250	Pullout
	$d_h = 38$	55	25	4.0	1.18	3.0	4.0	27	261	426	301	Splitting
	38 x 38	55	25	4.0	1.85	3.0	4.0	27	288	457	359	Splitting
	51 x 38	55	25	4.0	2.80	3.0	4.0	27	262	472 [‡]	384	Splitting
38 x 51	55	25	4.0	2.80	3.0	4.0	27	298	451	348	Splitting	
$d_h = 57$	55	25	4.0	4.04	3.0	4.0	21	209	319	284	Crushing	
51 x 51	55	25	4.0	4.06	3.0	4.0	21	240	385	308	Crushing	
76 x 38	55	25	4.0	4.70	3.0	4.0	28	321	472 [‡]	395	Yield	
76 x 38	55	25	4.0	4.70	3.0	4.0	21	359	459	366	Crushing	
38 x 76	55	25	4.0	4.70	3.0	4.0	27	335	472 [‡]	380	Splitting	
76 x 76	55	25	4.0	10.39	3.0	4.0	28	407	472 [‡]	409	Yield	
No head	45	25	4.0	0.00	3.0	4.0	28	83	300	188	Pullout	
$d_h = 38$	45	25	4.0	1.18	3.0	4.0	28	129	—	206	Splitting	
38 x 38	45	25	4.0	1.85	3.0	4.0	28	183	—	193	Splitting	
38 x 38	45	25	4.0	1.85	3.0	4.0	21	204	420	231	Splitting	
51 x 38	45	25	4.0	2.80	3.0	4.0	28	321	472	277	Yield	
51 x 38	45	25	4.0	2.80	3.0	4.0	21	259	412	236	Splitting	
38 x 51	45	25	4.0	2.80	3.0	4.0	27	339	459	266	Splitting	
$d_h = 57$	45	25	4.0	4.04	3.0	4.0	28	285	421	243	Yield	
51 x 51	45	25	4.0	4.06	3.0	4.0	21	304	459	279	Crushing	
76 x 38	45	25	4.0	4.70	3.0	4.0	21	370	413	229	Crushing	
38 x 76	45	25	4.0	4.70	3.0	4.0	27	336	472	284	Splitting	
76 x 76	45	25	4.0	10.39	3.0	4.0	21	—	376	204	Crushing	
76 x 76	45	25	4.0	10.39	3.0	4.0	26	377	472	265	Crushing	
Hook 1 [§]	45	25	4.0	—	3.0	4.0	28	—	—	218	Splitting	
Hook 2 [§]	45	25	4.0	—	3.0	4.0	28	—	—	235	Splitting	
No head	30	25	4.0	0.00	3.0	4.0	28	42	234	90	Pullout	
$d_h = 38$	30	25	4.0	1.18	3.0	4.0	28	206	412	138	Splitting	
38 x 38	30	25	4.0	1.85	3.0	4.0	28	279	472 [‡]	185	Yield	
$d_h = 57$	30	25	4.0	4.04	3.0	4.0	28	240	421 [‡]	168	Yield	
51 x 51	30	25	4.0	4.06	3.0	4.0	28	339	472 [‡]	181	Yield	
76 x 76	30	25	4.0	10.39	3.0	4.0	28	317	472 [‡]	173	Yield	
No head	45	36	4.0	0.00	2.8	3.0	28	94	268	304	Pullout	
$d_h = 52$	45	36	4.0	1.10	2.8	3.0	28	147	354	407	Splitting	
51 x 51	45	36	4.0	1.56	2.8	3.0	28	208	370	400	Splitting	
76 x 51	45	36	4.0	2.85	2.8	3.0	28	209	345	349	Splitting	
51 x 76	45	36	4.0	2.85	2.8	3.0	28	282	375	399	Crushing	
$d_h = 76$	45	36	4.0	3.53	2.8	3.0	28	254	385	417	Crushing	
102 x 51	45	36	4.0	4.13	2.8	3.0	28	390	427	428	Crushing	
51 x 102	45	36	4.0	4.13	2.8	3.0	28	269	393	395	Splitting	
76 x 76	45	36	4.0	4.77	2.8	3.0	28	274	392	374	Crushing	

Table 1—Summary of CCT node tests (continued)

	Head dimensions, mm*	θ_{strut} , degrees	d_b , mm	L_{plate}/d_b	A_{nh}/A_b	c/d_b	c_2/d_b	f'_c , MPa	f_s at $1d_b$, MPa	f_s at $7d_b$, MPa	P_{max} , kN	Failure mode
Unconfined tests (continued)	102 x 76	45	36	4.0	6.69	2.8	3.0	28	379	433 [‡]	426	Yield
	76 x 102	45	36	4.0	6.69	2.8	3.0	28	276	433 [‡]	441	Yield
	102 x 102	45	36	4.0	9.26	2.8	3.0	28	348	433 [‡]	479	Yield
Confined tests	No head	45	25	4.0	0.00	3.0	4.0	26	14	297	180	Pullout
	No head [#]	45	25	4.0	0.00	3.0	4.0	26	49	284	185	Pullout
	38 x 76	45	25	4.0	4.70	3.0	4.0	26	252	442	259	Splitting
	38 x 76 [#]	45	25	4.0	4.70	3.0	4.0	26	260	459	303	Splitting
	Hook 2 [§]	45	25	4.0	—	3.0	4.0	26	—	411	234	Splitting
	38 x 76 ^{**}	45	25	4.0	4.70	3.0	4.0	28	—	—	—	Pullout
	38 x 76 ^{††}	45	25	4.0	4.70	3.0	4.0	28	285	400	244	Crushing
	76 x 38 ^{‡‡}	45	25	4.0	4.70	3.0	4.0	26	377	455	261	Splitting

*Diameter (d_h) is given for circular heads. For rectangular heads, dimensions are given in order horizontal x vertical.

†Shear failure occurred in preliminary tests because insufficient stirrup reinforcement was provided to back (nontest) portion of specimen.

‡Bar stress is equal to f_y .

§Two 180 degree hooked bar details were tested: one in which beginning of bend was aligned with edge of bearing plate and one in which inside face of bend was aligned with edge of bearing plate. Refer to Reference 1 for additional details.

||10 mm-diameter stirrups placed in nodal region at 152 mm on center.

#10 mm-diameter stirrups placed in nodal region at 76 mm on center.

**Spiral reinforcement around head used as confinement: 76 mm bend diameter, 25 mm pitch, 4.8 mm diameter, and plain wire. Spiral prevented proper placement of concrete around head resulting in large void. Premature anchorage failure occurred.

††Special reinforcement placed along strut to hold strain gauges perpendicular to plain of strut-and-tie model. Refer to Reference 1 for further details.

‡‡Special reinforcement placed along strut gauges parallel to plain of strut-and-tie model. Refer to Reference 1 for further details.

Table 2—Unconfined CCT node database

No.	Head dimensions, mm	θ_{strut} , degrees	d_b , mm	L_{plate}/d_b	A_{nh}/A_b	c/d_b	c_2/d_b	f'_c , MPa	f_s at $1d_b$, MPa	f_s at $7d_b$, MPa	P_{max} , kN	Failure mode
1	No head	55	25	4.0	0.00	3.0	4.0	27	81	346	250	Pullout
2	$d_h = 38$	55	25	4.0	1.18	3.0	4.0	27	261	426	301	Splitting
3	38 x 38	55	25	4.0	1.85	3.0	4.0	27	288	457	359	Splitting
4	51 x 38	55	25	4.0	2.80	3.0	4.0	27	262	472	384	Splitting
5	38 x 51	55	25	4.0	2.80	3.0	4.0	27	298	451	348	Splitting
6	$d_h = 57$	55	25	4.0	4.04	3.0	4.0	21	219	319	284	Crushing
7	51 x 51	55	25	4.0	4.06	3.0	4.0	21	240	385	308	Crushing
8	76 x 38	55	25	4.0	4.70	3.0	4.0	21	359	459	366	Crushing
9	38 x 76	55	25	4.0	4.70	3.0	4.0	27	335	472	380	Splitting
10	No head	45	25	4.0	0.00	3.0	4.0	28	83	300	188	Pullout
11	$d_h = 38$	45	25	4.0	1.18	3.0	4.0	28	128	—	206	Splitting
12	38 x 38	45	25	4.0	1.85	3.0	4.0	28	183	—	193	Splitting
13	38 x 38	45	25	4.0	1.85	3.0	4.0	21	204	420	231	Splitting
14	51 x 38	45	25	4.0	2.80	3.0	4.0	21	259	412	236	Splitting
15	38 x 51	45	25	4.0	2.80	3.0	4.0	27	339	459	266	Splitting
16	51 x 51	45	25	4.0	4.06	3.0	4.0	21	304	459	279	Crushing
17	76 x 38	45	25	4.0	4.70	3.0	4.0	21	370	413	229	Crushing
18	38 x 76	45	25	4.0	4.70	3.0	4.0	27	336	472	284	Splitting
19	76 x 76	45	25	4.0	10.39	3.0	4.0	21	—	376	204	Crushing
20	76 x 76	45	25	4.0	10.39	3.0	4.0	26	377	472	265	Crushing
21	No head	30	25	4.0	0.00	3.0	4.0	28	42	234	90	Pullout
22	$d_h = 38$	30	25	4.0	1.18	3.0	4.0	28	206	412	138	Splitting
23	No head	45	36	4.0	0.00	2.8	3.0	28	94	268	304	Pullout
24	$d_h = 52$	45	36	4.0	1.10	2.8	3.0	28	147	354	407	Splitting
25	51 x 51	45	36	4.0	1.56	2.8	3.0	28	208	370	400	Splitting
26	76 x 51	45	36	4.0	2.85	2.8	3.0	28	209	345	349	Splitting
27	51 x 76	45	36	4.0	2.85	2.8	3.0	28	282	375	399	Crushing
28	$d_h = 76$	45	36	4.0	3.53	2.8	3.0	28	254	385	417	Crushing
29	102 x 51	45	36	4.0	4.13	2.8	3.0	28	390	427	428	Crushing
30	51 x 102	45	36	4.0	4.13	2.8	3.0	28	269	393	395	Splitting
31	76 x 76	45	36	4.0	4.77	2.8	3.0	28	274	392	374	Crushing

Table 3—Summary of statistical results for CCT node data

Model	Measured/calculated values			
	Range	Mean	Standard deviation	COV, %
Node overstress (ACI A.5)	1.60 to 10.9	5.57	2.37	42.4
Strut overstress (ACI A.3)	1.70 to 3.32	2.42	0.53	22.1
<i>Head-bearing component</i>				
Side blowout (ACI D.5.4)	0.87 to 1.69	1.25	0.23	18.0
Bearing strength (ACI 10.17)	0.66 to 1.35	0.93	0.18	19.3
Proposed model*	0.93 to 1.89	1.33	0.24	18.0
<i>Bond component</i>				
Peak bond	1.31 to 2.98	1.94	0.46	23.9
Failure bond	0.38 to 2.90	1.64	0.60	36.8

*Reduction factor of 0.7 applied.

of 1.0 is used for the concrete strength f'_c (as with the bearing model), and a term is included that relates capacity to the ratio c_2/c (as with the side-blowout model). The parameters of each model are summarized in Table 4.

The proposed model was optimized against a database consisting of published data from bearing tests and tests of deeply embedded anchor bolts and headed reinforcement. The headed anchor and headed reinforcing bar tests comprised a set of side blowout failures. Bearing tests are typically conducted on concrete blocks that fail by splitting. Mixing of these test results is based on the contention that these two failure modes initiate from the same cause, the formation of a driving wedge in front of the bearing surface that causes lateral splitting stress (refer to Fig. 3). The sources used for the database and the ranges of significant variables are listed in Table 5. The significant parameters for calculating bearing pressure are $2c/\sqrt{A_{nh}}$ (equivalent to $\sqrt{A_2/A_1}$ used in ACI 318, Section 10.17), c_2/c , and f'_c . The database is composed of 69% bearing failures and 31% side blowout failures. The test data included in the database were required to meet the following criteria:

- Failure of the concrete by side blowout or splitting must have occurred. Tests of anchor bolts or headed bars in which steel fracture or yielding was the listed cause of failure were omitted;
- Headed bar data must be for head capacity only. The bond component of anchorage must be excluded. Thus, either the data for bar stress at the head was provided in the published data or bond was prevented by a sheath around the bar during the test;
- Anchor bolts or headed bars must have an embedment length greater than five times the least cover dimension. This depth-to-cover ratio should exclude concrete breakout failures;
- Double punch bearing tests were excluded. Additionally, the height of the bearing block had to be at least twice the side cover dimension;
- The bearing surface had to be rigid and the aspect ratio of the bearing surface (length/width) could not be greater than 2.1; and
- Only unconfined tests were considered. (This led to the omission of another possible test type from the database, post-tensioned anchorages. Though the behavior of post-tensioned anchorages was expected to match that of the other test types, the vast majority of post-tensioned anchorage tests include spiral confinement in front of

Table 4—Significant parameters of models for head capacity

Failure mode	Relation to significant variables			
	Concrete strength	Head-bearing area	Minimum side cover	Secondary side cover
Bearing	f'_c	$(A_1)^{0.5}$	$(A_2)^{0.5} \propto c$	—
Side blowout	$(f'_c)^{0.5}$	$(A_{nh})^{0.5}$	c	$(1 + c_2/c)/4$
Proposed	f'_c	$(A_{nh})^{0.5}$	c	$0.6 + 0.4(c_2/c)$

Definition of Significant Variables:

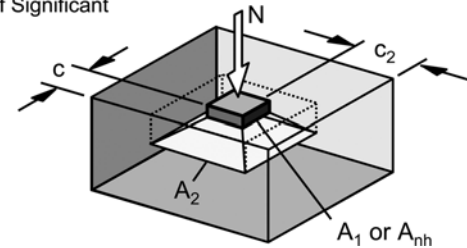


Table 5—Database of bearing and side blowout data

Source	Type of test	No. of data values	Ranges for variables		
			f'_c , MPa*	$2c/\sqrt{A_{nh}}$	c_2/c
DeVries ³	Headed bar	73	19 to 44	1.0 to 3.8	1.0 to 15.2
Current study	Headed bar	26	21 to 29	2.1 to 6.2	1.1 to 1.3
Breen ⁶	Anchor bolt	17	22 to 38	2.0 to 3.7	3.1 to 4.0
Lee and Breen ⁷	Anchor bolt	7	15 to 37	2.6 to 3.5	4.0 to 6.4
Hasselwander et al. ⁸	Anchor bolt	16	21 to 38	1.3 to 3.6	3.0 to 6.0
Hasselwander et al. ⁹	Anchor bolt	9	18 to 38	1.5 to 4.1	3.4 to 12.0
Furche and Eligehausen ¹⁰	Anchor bolt	20	26	2.9 to 7.4	3.8 to 7.5
Shelson ¹¹	Bearing block	12	39 to 46	2.8 to 8.0	1.0
Au and Baird ¹²	Bearing block	12	31 to 56	1.4 to 4.0	1.0
Hawkins ¹³	Bearing block	73	12 to 52	1.0 to 6.8	1.0 to 6.0
Niyogi ^{14,15}	Bearing block	119	10 to 50	1.0 to 8.0	1.0 to 4.0
Williams ¹⁶	Bearing block	159	18 to 68	1.0 to 10.2	1.0 to 9.4
All headed bar tests		99	19 to 44	1.0 to 6.2	1.0 to 15.2
All anchor bolt tests		69	15 to 38	1.3 to 7.4	3.0 to 12.0
All bearing block tests		375	10 to 68	1.0 to 10.2	1.0 to 9.4
All tests		543	10 to 68	1.0 to 10.2	1.0 to 15.2

*Cylinder strength or equivalent value.

the bearing surface, which can significantly affect behavior.)

Once the database was compiled, optimal exponents and coefficients for each variable were found. The form of the proposed model is

$$\text{Bearing pressure, } \frac{N}{A_{nh}} = 0.9f'_c \left(\frac{2c}{\sqrt{A_{nh}}} \right) \Psi \quad (1)$$

where Ψ (radial disturbance factor) = $0.6 + 0.4 \left(\frac{c_2}{c} \right) \leq 2.0$ (2)

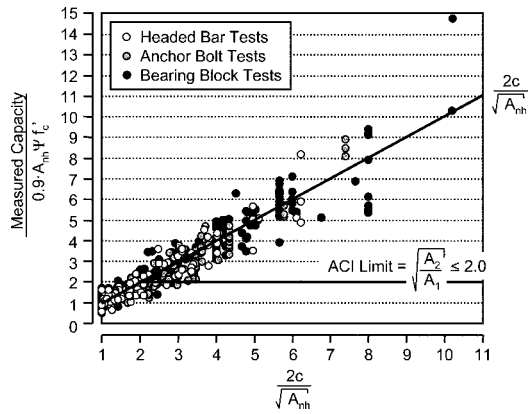


Fig. 4—Effects of ratio $2c/\sqrt{A_{nh}}$ on proposed model.

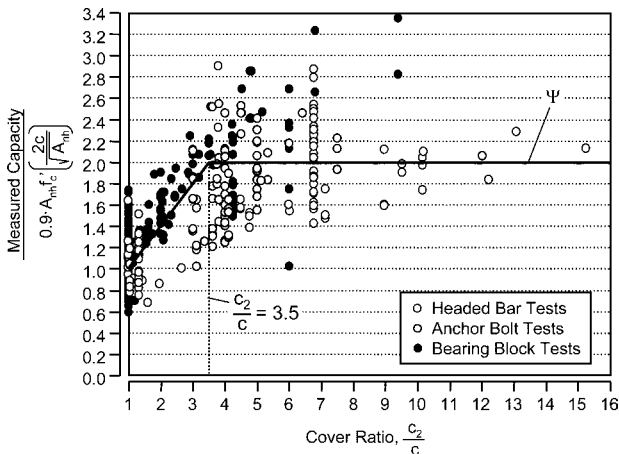


Fig. 5—Effect of cover ratio (c_2/c) on proposed bearing model.

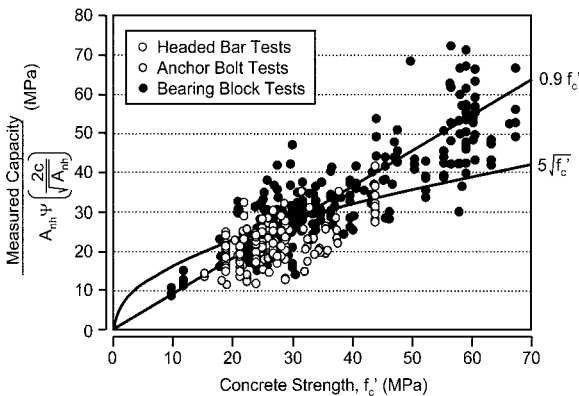


Fig. 6—Effect of concrete strength (f'_c) on proposed model.

The radial disturbance factor accounts for the effect of cover ratio. The title of this term has been used previously in anchor bolt studies and is used here for consistency.

The trends of the database and fit of the proposed model are illustrated in Fig. 4, 5, and 6. The effect of the $2c/\sqrt{A_{nh}}$ term is shown in Fig. 4. Capacity increased linearly in proportion to $2c/\sqrt{A_{nh}}$ well past the limit of 2 imposed by ACI 318, Section 10.17. Furthermore, the data for bearing tests, anchor bolts, and headed bars fell within the same band, indicating that the test types are indeed similar. The effect of the radial disturbance factor Ψ is shown in Fig. 5. Despite much scatter at $c_2/c \cong 3.5$, the average capacity was about double that at $c_2/c = 1$. The equation for the proposed

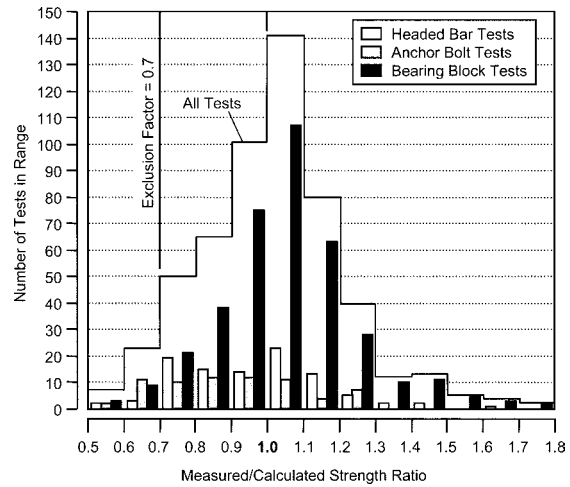


Fig. 7—Distribution plot from analysis of proposed model.

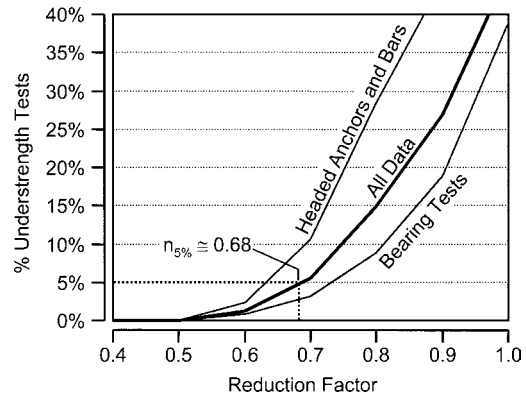


Fig. 8—Percent of unsafe tests as function of applied reduction.

radial disturbance factor was chosen to approximate this trend. The effect of concrete strength is shown in Fig. 6. The data were best described by a linear relationship to concrete strength (a best fit curve for a $\sqrt{f'_c}$ relationship is shown for comparison).

The distribution of measured strength to calculated strength ratios is shown in Fig. 7. Statistical results for the proposed model are summarized in Table 6. The distribution plot is dominated by bearing tests. The average measured/calculated value for bearing tests was 1.04 while the average value for headed anchors and headed bars was 0.94. There was approximately a 10% difference between the side-blowout failures and bearing failures. This can be seen in the distribution plot where headed bar and headed anchor data peak slightly to the left of bearing tests. The proposed model was developed to fit the mean of the data. For design, the model needs to be adjusted to include more tests in the safe range of measured/calculated values (≥ 1.0). The distribution plot was integrated to provide the percentage of tests excluded from a safe calculated outcome as a reduction factor was applied to the model. The result is plotted in Fig. 8. Using 5% as an acceptable limit of excluded test results, a factor of about 0.7 must be applied to the proposed model. (Note: This is not the same as a strength reduction ϕ factor.)

With the reduction factor applied, the database of 26 CCT node specimens was compared with the proposed model. The ranges, means, and coefficients of variation for this comparison are given in Table 3. The model provided a conservative estimate of bar stress at the head for all but one test.

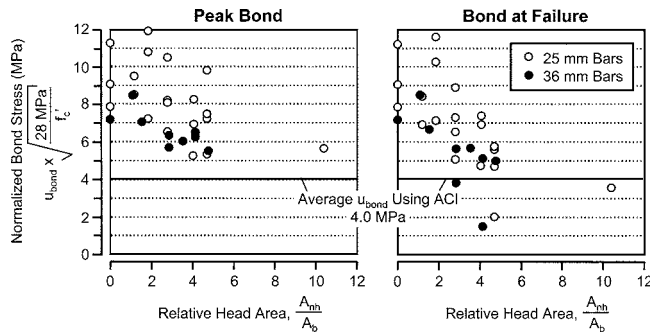


Fig. 9—Bond data plotted as function of relative head area.

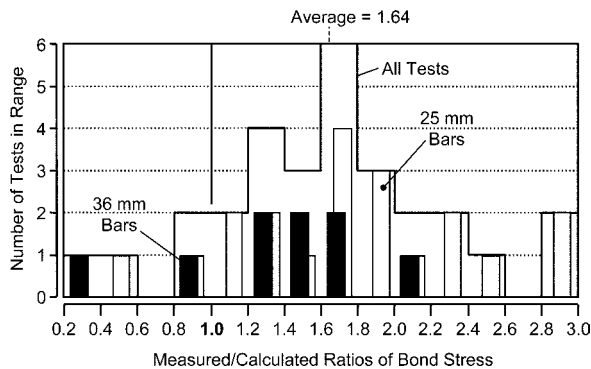


Fig. 10—Distribution plot from analysis of failure bond.

ANALYSIS OF BOND

Average bond stress was determined for the CCT node tests by using the difference between bar stress at $1d_b$ from the head and $7d_b$ from the head. Two values of average bond stress are significant for each test: the peak average bar stress and the average bond stress at failure. As summarized from Part 1,¹ bond tends to peak and then decline before anchorage failure of a headed bar occurs. These values were determined for 28 of the CCT nodes listed in Table 2 (Tests 11, 12, and 19 were excluded because bar stress data was lacking at key locations). Average bond stress (peak and failure) is plotted as a function of relative head area in Fig. 9. For comparison, the ACI development length equation, Eq. (12-1), was used to calculate theoretical average bond stress, which is also plotted.

Peak bond stress decreased with increasing head area. Furthermore, between peak and failure bond, there was an additional decrease in relation to increasing head area. The cause of the reduction between peak and failure bond was discussed in Part 1.¹ It is the result of the decline in bond as bar stress is transferred to the head. Peak bond probably decreases in relation to head size as a result of increased slip resistance in a headed bar versus a nonheaded bar. Head bearing provides a stiffer anchor than bond, thus attracting more bar stress to the head and preventing bond from developing fully, even when bond peaks. The combined effect of these reductions can lead to a significant drop in bond capacity at failure between a headed bar and a nonheaded bar.

Despite the reductions, most of the bond stresses measured at failure were greater than calculations with the ACI development length equation. The distribution of measured/calculated bond ratios is plotted in Fig. 10. Further analysis and discussion of bond in headed bars can be found in Reference 17. The existing database is considered too small to develop a complete model for bond in headed reinforcement.

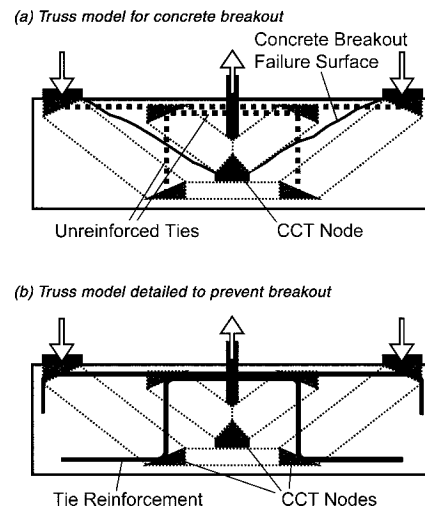


Fig. 11—Truss model for concrete breakout.

Table 6—Statistical results for proposed bearing model

Source	Measured/calculated values			
	Range	Mean	Standard deviation	COV, %
DeVries ³	0.53 to 1.63	0.98	0.21	21.3
Current study	0.65 to 1.32	0.93	0.17	18.0
Breen ⁶	0.55 to 1.27	0.83	0.21	25.2
Lee and Breen ⁷	0.62 to 1.23	0.93	0.20	21.3
Hasselwander et al. ⁸	0.60 to 1.26	0.93	0.24	25.5
Hasselwander et al. ⁹	0.64 to 1.03	0.80	0.14	17.8
Furche and Eligehausen ¹⁰	0.77 to 1.21	0.98	0.11	11.7
Shelson ¹¹	0.67 to 1.02	0.81	0.12	14.9
Au and Baird ¹²	0.77 to 1.24	0.99	0.16	15.7
Hawkins ¹³	0.71 to 1.73	1.10	0.21	19.3
Niyogi ^{14,15}	0.63 to 1.50	1.03	0.14	13.4
Williams ¹⁶	0.50 to 1.68	1.05	0.20	19.5
All headed bar tests	0.53 to 1.63	0.97	0.20	20.6
All anchor bolt tests	0.55 to 1.27	0.90	0.19	21.3
All bearing block tests	0.50 to 1.73	1.04	0.19	18.2
All tests	0.50 to 1.73	1.01	0.20	19.6

DISCUSSION

Anchorage failure

Within the nodal zone, anchorage of tie bars must be satisfied. Anchorage has no specific definition in the ACI code and is a concept that simply implies an adequate connection between steel reinforcing elements and the concrete mass to which they are connected. There are many failure modes associated with anchorage: crushing of concrete or spalling at a post-tensioned anchorage zone (ACI 318, Section 18.13), concrete breakout of an anchor bolt (ACI 318, Section D.5.2), side blowout of an anchor bolt (ACI 318, Section D.5.4), and bond failure (ACI 318, Section 12.2). This study has dealt with crushing (bearing strength) of concrete, side blowout, and bond failure, but not concrete breakout. This is not an oversight. When the STM process is properly applied, concrete breakout will be recognized as a failure of ties within the truss mechanism (Fig. 11). As a possible failure mode, it has nothing to do with the CCT

(a) Elastic lateral stress profile (b) Truss model

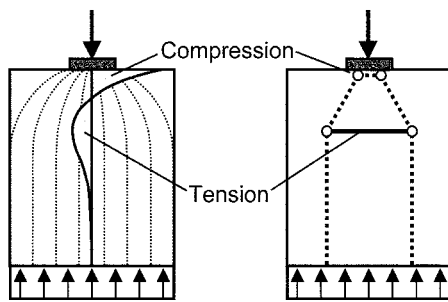


Fig. 12—Truss mechanism for spreading of concentrated stress.

node at the anchor head. Concrete breakout occurs for anchors because reinforcement has not been provided to redirect the stress path back into the mass of the concrete. As a consequence, a truss mechanism forms that relies on concrete in tension to fill the role of the ties. In any STM analysis, concrete breakout is not a failure mode of the node. It is an issue of the overall truss mechanism. (Note: anchorage failure at the bottom CCT nodes within the truss mechanism drawn in Fig. 11(b) could result in a failure that resembles concrete breakout. Failure capacity in such a case, however, would be a function of development length of the tie reinforcement at those CCT nodes or other node anchorage criteria.)

Failure of node or struts

Failure of the CCT nodes studied in this research could be modeled with reasonable accuracy using the proposed model for head-bearing capacity. It is believed that a check of anchorage capacity (which would include head bearing) is sufficient to determine the capacity of CCT nodes anchored by headed reinforcement without the additional calculations based on node face stress currently required under ACI 318, Section A.5. Additionally, the requirements for calculating strut capacity under ACI 318, Section A.3 were found to be unnecessary for the specimens studied. Evidence from specially instrumented specimens (discussed in Part 1¹) showed that failure initiated from conditions at the ends of the strut (at the nodes), which can in turn be related primarily to head bearing. Once head bearing is checked during the calculation of anchorage capacity for a headed bar, capacity of the node should be satisfied and capacity of the strut may also be satisfied. This recommendation is limited by the scope of the test program, which includes primarily unconfined CCT nodes.

Support for the idea that the strut capacity can be satisfied by a check of head bearing comes from related research by Adebar and Zhou.¹⁸ They studied the capacity of isolated struts analytically and experimentally. Their experimental specimens were plain, unreinforced concrete cylinders loaded through rigid bearing plates at both ends. They found the capacity of these struts to be related to the concrete strength f'_c , the square root of the ratio of the bearing area of the load plate to the area of the strut $\sqrt{A_2/A_{nh}}$, and the aspect ratio of the strut h/b —the length of the strut along its axis of force divided by its minimum width.

$$\text{Bearing pressure, } \frac{N}{A_{nh}} = 0.6f'_c(1 + 2\alpha\beta) \quad (3)$$

$$\text{where } \alpha = 0.33 \left(\sqrt{\frac{A_2}{A_{nh}}} - 1 \right) \leq 1.0 \quad (4)$$

$$\beta = 0.33 \left(\frac{h}{b} - 1 \right) \leq 1.0 \quad (5)$$

With the exception of h/b , the model for strut capacity is dependent on many of the same parameters found to describe the capacity of CCT nodes in this study.

The reason that similar models were found for the nodes and struts of this study and Adebar and Zhou's¹⁸ is because both models are addressing the same mechanism of failure, splitting caused by spreading of stress from a concentrated area to the full width of the strut (refer to Fig. 12). At either end of the strut, the stress path from the body of the strut must generally compact itself to be compatible with tie bars or bearing plates. Lateral splitting stress will result at the locations where the strut must transition from a larger width to a smaller one near the ends of the strut. Splitting stress was the cause of failure in many of the specimens from this study. The model developed in this paper (Eq. (1) and (2)) provides the bearing capacity associated with failure caused by this transition and associated splitting stress. The model accurately calculated failure of struts/CCT nodes anchored by headed reinforcement. A similar model (using bond stress perhaps) may describe failure of struts/CCT nodes anchored by more conventional reinforcement. If so, analysis of nodes and struts in STM could be simplified by focusing on fewer modes of failure.

Bond in headed reinforcement

Anchorage of the tie bar to the node can occur by bond, head bearing, or hook bearing and must occur within the length provided by the extended CCT nodal zone. For the headed reinforcement tests conducted in this study, anchorage was a combination of bond and head bearing (with head bearing providing the majority of anchorage capacity in most cases). The bond component of anchorage was poorly modeled using the existing ACI development length equation. Presently, there is little data upon which to develop a complete picture of bond in headed reinforcement. Because bond provided only a fraction of the anchorage capacity for the headed reinforcement tested in this study, however, it was of less consequence that an accurate model was found. The topic of bond in headed reinforcement is left unresolved with this study, but should be pursued in subsequent research.

CONCLUSIONS

CCT nodes anchored by headed reinforcement fail when bearing capacity at the head reaches a limit described by the following

$$\text{Bearing pressure, } \frac{N}{A_{nh}} = 0.9f'_c \left(\frac{2c}{\sqrt{A_{nh}}} \right) \Psi$$

$$\text{where } \Psi = 0.6 + 0.4 \left(\frac{c_2}{c} \right) \leq 2.0$$

Compatibility requires concentrated stress at the bearing plate to spread across the full width available to the strut at

midlength. This spreading causes lateral tension just outside of the nodal zone that can be modeled as a tie across unreinforced concrete. Failure of the node and strut occurs when this tie ruptures. The current data suggest that a calculation of anchorage capacity using the proposed bearing strength model is sufficient to check capacity of the node and strut. The methods recommended in ACI 318, Appendix A, involving stress limits at node and strut faces, were overly conservative for the CCT node specimens tested in this research.

Bond capacity corresponding to anchorage failure of a headed bar decreases with increasing relative head area. The current bond data was poorly modeled using the development length equation of ACI 318, Section 12.2.3. The current data is too limited to suggest an appropriate model for bond in headed reinforcement. Additional research into this topic is suggested.

A summary of statistical results for the models analyzed against the CCT node data is presented in Table 3.

ACKNOWLEDGMENTS

The support of the Texas Department of Transportation and the guidance of the project supervisor D. Van Landuyt is gratefully acknowledged. The test program was conducted at the Ferguson Structural Engineering Laboratory of the University of Texas at Austin, Austin, Tex. The help of the laboratory staff and special efforts of graduate students M. Ziehl and A. Ledesma were essential to the conduct of the study.

NOTATION

A_1	=	net bearing area of rigid bearing plate, alternative notation for A_{nh} (ACI 318, Section 10.17), mm ²
A_2	=	area of frustum created when pyramid is projected from bearing face to closest free edge, mm ²
A_b	=	bar area, mm ²
A_{gh}	=	gross head area, mm ²
A_{nh}	=	net head area, $A_{gh} - A_b$, mm ²
b	=	minimum lateral width of strut measured perpendicular to line of force, mm
c	=	minimum cover dimension, measured to bar center, mm
c_2	=	minimum cover dimension, measured in direction orthogonal to c , mm
d_b	=	bar diameter, mm
f'_c	=	concrete compression strength, from cylinder tests, MPa
f_s	=	bar stress, in general, MPa
$f_{s,bond}$	=	bar stress provided by bond, MPa
$f_{s,head}$	=	bar stress provided by head bearing, MPa
h	=	length of strut along the line of force, mm
N	=	bearing strength capacity, kN
$n_{5\%}$	=	reduction applied to capacity so only 5% of test data fail to be calculated conservatively
P	=	bearing reaction at CCT node, kN
u_{bond}	=	average bond stress along bar, MPa
θ_{strut}	=	strut angle, measured between axis of tie bar and axis of strut
Ψ	=	radial disturbance factor, $0.6 + 0.4(c/c_2) \leq 2.0$

REFERENCES

1. Thompson, M. K.; Ziehl, M. J.; Jirsa, J. O.; and Breen, J. E., "CCT Nodes Anchored by Headed Bars—Part 1: Behavior of Nodes," *ACI Structural Journal*, V. 102, No. 6, Nov.-Dec. 2005, pp. 808-815.
2. ACI 318-02, "Building Code Requirements for Structural Concrete (ACI 318-02) and Commentary (318R-02)," American Concrete Institute, Farmington Hills, Mich., 2002, 443 pp.
3. DeVries, R. A., "Anchorage of Headed Reinforcement in Concrete," PhD dissertation, The University of Texas at Austin, Austin, Tex., Dec. 1996, 314 pp.
4. DeVries, R. A.; Jirsa, J. O.; and Bashandy, T., "Effects of Transverse Reinforcement and Bonded Length on the Side-Blowout Capacity of Headed Reinforcement," *Bond and Development Length of Reinforcement: A Tribute to Peter Gergely*, SP-180, R. Leon, ed., American Concrete Institute, Farmington Hills, Mich., 1998, pp. 367-389.
5. Thompson, M. K.; Young, M. J.; Jirsa, J. O.; Breen, J. E.; and Klingner, R. E., "Anchorage of Headed Reinforcement in CCT Nodes," *Center for Transportation Research Report* 1855-2, Austin, Tex., May 2002, 160 pp.
6. Breen, J. E., "Development Length for Anchor Bolts," *Center for Transportation Research Report* CTR-55-1F, Austin, Tex., Apr. 1964.
7. Lee, D. W., and Breen, J. E., "Factors Affecting Anchor Bolt Development," *Center for Transportation Research Report* CTR-88-1F, Austin, Tex., Aug. 1966.
8. Hasselwander, G. B.; Jirsa, J. O.; Breen, J. E.; and Lo, K., "Strength and Behavior of Anchor Bolts Embedded Near Edges of Concrete Piers," *Center for Transportation Research Report* CTR-29-2F, Austin, Tex., May 1977.
9. Hasselwander, G. B.; Jirsa, J. O.; and Breen, J. E., "Strength and Behavior of Single Cast-in-Place Anchor Bolts Subject to Tension," *Proceedings of the International Symposium Anchorage to Concrete*, SP-103, G. B. Hasselwander, ed., American Concrete Institute, Farmington Hills, Mich., 1984, pp. 203-231.
10. Furche, J., and Eligehausen, R., "Lateral Blow-Out Failure of Headed Studs Near a Free Edge," *Anchors in Concrete—Design and Behavior*, SP-130, G. A. Senkiw and H. B. Lancelot III, eds., American Concrete Institute, Farmington Hills, Mich., 1991, pp. 235-252.
11. Shelson, W., "Bearing Capacity of Concrete," *ACI JOURNAL, Proceedings* V. 54, No. 5, Nov. 1957, pp. 405-414.
12. Au, T., and Baird, D. L., "Bearing Capacity of Concrete Blocks," *ACI JOURNAL, Proceedings* V. 56, No. 9, Mar. 1960, pp. 869-879.
13. Hawkins, N. M., "The Bearing Strength of Concrete: 1—Loading Through Rigid Plates Covering Part of the Full Supporting Area," *Research Report* No. 54, The University of Sydney, Sydney, Australia, Mar. 1967, 46 pp.
14. Niyogi, S. K., "Bearing Strength of Concrete—Geometric Variations," *Journal of Structural Engineering*, ASCE, V. 99, No. 7, July 1973, pp. 1471-1490.
15. Niyogi, S. K., "Concrete Bearing Strength—Support, Mix, Size Effect," *Journal of Structural Engineering*, ASCE, V. 100, No. 8, Aug. 1974, pp. 1685-1702.
16. Williams, A., "The Bearing Capacity of Concrete Loaded Over a Limited Area," *Technical Report* 526, Cement and Concrete Association, Wexham Springs, Slough, UK, Aug. 1979, 70 pp.
17. Thompson, M. K.; Ledesma, A. L.; Jirsa, J. O.; Breen, J. E.; and Klingner, R. E., "Anchorage Behavior of Headed Reinforcement," *Center for Transportation Research Report* 1855-3, Austin, Tex., May 2002, 122 pp.
18. Adebar, P., and Zhou, Z., "Bearing Strength of Compressive Struts Confined by Plain Concrete," *ACI JOURNAL, Proceedings* V. 90, No. 5, Sept.-Oct. 1993, pp. 534-541.
19. Thompson, M. K.; Jirsa, J. O.; Breen, J. E.; and Klingner, R. E., "Anchorage Behavior of Headed Reinforcement: Literature Review," *Center for Transportation Research Report* 1855-1, Austin, Tex., May 2002, 112 pp.